CANCER BIOTHERAPY & RADIOPHARMACEUTICALS
Volume 19, Number 2, 2004

PET Radioimmunoscintigraphy of Renal Cell Cancer Using ^{89}Zr-Labeled cG250 Monoclonal Antibody in Nude Rats

Adrienne Brouwers,[1] Iris Verel,[2] Julliëtte Van Eerd,[1] Gerard Visser,[3] Martijn Steffens,[4] Egbert Oosterwijk,[4] Frans Corstens,[1] Wim Oyen,[1] Guus Van Dongen,[2] and Otto Boerman[1]
Departments of Nuclear Medicine[1] and Urology,[4] University Medical Center Nijmegen, Nijmegen, The Netherlands
Department of Otolaryngology/Head and Neck Surgery,[2] VU University Medical Center, and Radionuclide Center,[3] VU University, Amsterdam, The Netherlands

ABSTRACT

Introduction: *With the introduction of positron-emitting radionuclides with half-lifes in days, such as ^{89}Zr and ^{124}I, radioimmunoscintigraphy (RIS) with positron-emitter-labeled monoclonal antibodies (moAbs) becomes feasible. RIS, using positron emission tomography (immuno-PET), combines the specific localization of an antibody with the high resolution of a PET camera. In the present study, scintigraphic tumor imaging using chimeric moAb G250 labeled with ^{89}Zr (immuno-PET) or ^{111}In (RIS), and [^{18}F]FDG-(PET) was explored in rats with s.c. renal cell carcinoma (RCC) tumors.*
Methods: *Nude rats (6–8 rats per group) with s.c. SK-RC-52 tumors were i.v. injected with 4 MBq ^{111}In-DTPA-cG250, 20 MBq ^{89}Zr-Df-cG250 or 4 MBq [^{18}F]FDG. Planar ^{111}In-DTPA-cG250 images were obtained 5 minutes, and 24, 48, and 72 hours postinjection (p.i.). 3D PET imaging was performed 5 minutes, and 24, 48, and 72 hours after a ^{89}Zr-Df-cG250 injection and 1 hour after a [^{18}F]FDG injection using a Siemens ECAT EXACT PET camera. Rats were killed after the last imaging session, and the uptake of the radiolabel in the dissected tissues was determined.*
Results: *Both radiolabeled antibody preparations were stable during 4 days of incubation in serum at 37°C, and the immunoreactivity was preserved. Two (2) days after injection, s.c. tumors (100 mg) were clearly visualized, both with ^{89}Zr-Df-cG250 and ^{111}In-DTPA-cG250. Tumors were not visualized with [^{18}F]FDG (uptake in tumor of 0.5 ± 0.1 %ID/g, 1 hour p.i.). The biodistribution experiments showed an identical uptake in the tumor for both ^{89}Zr-Df-cG250 and ^{111}In-DTPA-cG250 at 3 days p.i. (5.0 ± 2.4 and 4.9 ± 2.9 %ID/g, respectively). Blood levels at 3 days p.i. were also identical (1.4 ± 0.4 versus 1.7 ± 0.7 %ID/g), and no significant differences were found in the biodistribution of normal tissues between the two radiolabeled cG250 preparations.*
Conclusion: *The cG250 antibody can be stably labeled with the positron-emitter ^{89}Zr, while preserving the immunoreactivity of the moAb. In this rat model, the* in vivo *biodistribution of ^{89}Zr-Df-cG250 was identical to that of ^{111}In-DTPA-cG250. Immuno-PET of RCC is feasible with ^{89}Zr-cG250, and relatively small tumors could be visualized, even without a dedicated PET camera for small animals.*

Key words: ^{89}Zr, positron emission tomography, monoclonal antibody cG250, renal cell carcinoma, radioimmunoscintigraphy

Address reprint requests to: Otto Boerman; Department of Nuclear Medicine, University Medical Center Nijmegen; P.O. Box 9101, 6500 HB Nijmegen, The Netherlands; Tel.: +31-24-3613813; Fax: +31-24-3618942
E-mail: o.boerman@nucmed.umcn.nl

INTRODUCTION

Whole-body positron emission tomography (PET) offers some major advantages over whole-body

scintigraphy with a gamma camera: (1) better detection of smaller lesions resulting from better spatial and temporal resolution, (2) more accurate localization of lesions owing to 3-dimensional (3D) information, and (3) a more accurate quantitative estimation of the uptake, allowing for more reliable radiation dose estimates.

PET imaging with [^{18}F]FDG is based on an enhanced glucose uptake by malignant cells. Whereas, for a lot of malignancies, the role of [^{18}F]FDG-PET for the diagnosis, staging, and more recently, assessing a response to treatment, is evolving; for renal cell carcinoma (RCC), the potential of [^{18}F]FDG-PET is less well defined.[1] RCC lesions in the abdomen may be difficult to detect, because of the physiological accumulation of FDG in the urinary tract. Reports on [^{18}F]FDG-PET in RCC patients are scarce, and cover relatively small numbers of patients.[2–4]

There is a renewed interest in radioimmunoscintigraphy (RIS) using positron emitters, also designated as immuno-PET, for the visualization of tumors. One of the reasons for this is the rapidly expanding number of PET scanners. However, the development of immuno-PET is still in an early phase, mainly because the half-life of most commonly used positron emitters (^{11}C, ^{18}F, ^{15}O, and ^{13}N) is too short for use with antibodies *in vivo*. This applies also for positron emitters, such as ^{64}Cu and ^{86}Y, with half-lifes ($t_{1/2}$) of 12.7 and 14.7 hours, respectively. Positron emitters like ^{89}Zr and ^{124}I with a half-life of 78 and 100 hours better match the relatively slow pharmacokinetics of radiolabeled monoclonal antibodies (moAbs) (optimal uptake in tumor lesions is usually reached after several days for whole IgGs). PET imaging of tumors with positron emitters labeled to moAbs could be of particular interest not only for visualization and staging, but also for dose planning in radioimmunotherapy (RIT).[5] A method for the stable coupling of the positron emitter ^{89}Zr to moAbs was developed by Meijs et al.[6] and further improved by Verel et al.[7] MoAbs could be easily and stably radiolabeled with zirconium via a desferal analogue that can be coupled to moAbs, *N*-succinyldesferrioxamine B (*N*-sucDf). ^{89}Zr-Df labeled to chimeric (c) moAb U36, directed against head and neck cancer, showed excellent *in vitro* stability.[7] *In vivo*, ^{89}Zr after release from the chelate may incorporate into the bone, as is also observed for other metallic radionuclides, such as ^{90}Y and ^{177}Lu.[8–10] Therefore, stable labeling is crucial. High specific tumor accumulation in HNX-OE tumors in nude mice was demonstrated with ^{89}Zr-Df-cU36. Small tumors (19–154 mg) were clearly visualized with a prototype animal PET scanner.[7]

In our group, we have ample experience with RIS and RIT, using chimeric human/mouse moAb G250 targeting RCC.[11,12] The aim of this study was to explore immuno-PET with ^{89}Zr-Df-cG250. The radiolabeling characteristics of ^{89}Zr-Df-cG250, the biodistribution, and its performance as a PET imaging tracer were studied in nude rats with subcutaneous (s.c.) RCC xenografts. In addition, in the same nude rat model, the *in vivo* characteristics of ^{111}In-labeled cG250 (RIS) and [^{18}F]FDG (FDG-PET) were studied and compared to those of ^{89}Zr-Df-cG250.

MATERIAL AND METHODS

Chimeric Monoclonal Antibody G250

The isolation and the immunohistochemical reactivity of moAb G250 have been described elsewhere.[11,12] MoAb cG250 is reactive with the antigen G250 ($K_a = 4 \times 10^9\ M^{-1}$), being the tumor-associated isoenzyme carbonic anhydrase isoenzyme IX (MN/CA IX).[13] It is expressed on the cell surface of nearly all clear cell RCCs, and is absent on most normal tissues and other malignancies.[11,12,14,15]

Conjugation, Radiolabeling, and Quality Control

The conjugation of *N*-succinyldesferrioxamine B (*N*-sucDf) to moAb cG250 was performed, as has been described previously.[7] Briefly, desferal (Novartis Pharma AG, Bern, Switzerland) was succinylated (*N*-sucDf), temporarily filled with Fe^{3+}, and coupled to cG250 via the tetrafluorophenol-N-sucDf-ester. After the conjugation of Df to the moAb, the removal of the Fe^{3+} and the labeling of the Df-conjugated moAb with ^{89}Zr,[16] the conjugate was purified on a PD-10 column (Amersham Pharmacia Biotech, Uppsala, Sweden), using 0.9% NaCl + 5 mg/mL of gentisic acid, with a pH of 5.0, as the eluent. Df-cG250 (0.37 mg) was labeled with 165 MBq of ^{89}Zr during 30 minutes in 0.25 M HEPES buffer, with a pH of 7.3.

cG250 was conjugated with isothiocyanato-benzyl-diethylenetriaminepentaacetic acid (SCN-Bz-DTPA) (Macrocyclics, Richardson, TX) in a 0.1 M $NaHCO_3$ buffer, with a pH of 8.5, using a fifty-fold (SCN-Bz-DTPA) molar excess, as described

by Ruegg et al., with a minor modification (a conjugation period of 1 hour at room temperature).[17] Unconjugated DTPA was removed from the moAb preparation by extensive dialysis against 0.25 M of ammonium acetate buffer, with a pH of 5.4. The cG250-DTPA conjugate was labeled with $^{111}InCl_3$ (Tyco Healthcare, Petten, The Netherlands) in 0.25 M of ammonium acetate buffer, with a pH of 5.4 (30 minutes at room temperature). The ^{111}In-cG250 preparation was purified on a PD-10 column, using phosphate buffered saline (PBS), supplemented with 0.5% of the bovine serum albumin (BSA) as the eluent. The number of *N*-sucDf or DTPA ligands per cG250-molecule was determined as described by Verel et al.[7] and Hnatowich et al.,[18] respectively.

The radiochemical purity of the radiolabeled cG250 preparations was determined by instant thin layer chromatography (ITLC), using ITLC silica gel strips (Gelman Sciences, Inc., Ann Arbor, MI), and 0.1 M of citrate buffer (pH 6.0) for ^{111}In-DTPA or 0.02 M of citrate buffer (pH 5.0) for ^{89}Zr-Df-cG250 as the mobile phase.

At the time of intravenous (i.v.) injection, the immunoreactive fraction at infinite antigen excess of the radiolabeled cG250 preparations was determined on freshly trypsinized SK-RC-52 RCC cells, essentially as described by Lindmo et al., with minor modifications.[12,19]

To assess the stability of the ^{111}In- and ^{89}Zr-labeled preparations, both the ^{111}In- and ^{89}Zr-labeled MoAb preparations were diluted in human plasma at an activity concentration of 1.8 MBq/mL. A final concentration of 0.5 mM ethylenediaminetetraacetic acid (EDTA) was added to capture released radiometal, and the preparations were incubated at 37°C. Plasma samples of both ^{89}Zr-Df-cG250 and ^{111}In-DTPA-cG250 were analyzed at 0 and 4 hours and 1, 2, and 4 days of incubation by fast protein liquid chromatography (FPLC), using a Biosep Sec-S3000 gel filtration column (Phenomenex, Torrace, CA). The column was calibrated with IgG (R_f = 11 minutes), transferrin (R_f = 12 minutes), ^{111}In (R_f = 17 minutes), and ^{111}In-DTPA (R_f = 17 minutes).

^{18}F-Labeled Deoxyglucose

Clinical grade [^{18}F]FDG was purchased from Tyco Healthcare, Petten, The Netherlands.

Nude Rats Tumor Model

The RCC cell line SK-RC-52 was derived from a mediastinal metastasis of a primary RCC, and has been described elsewhere.[20] SK-RC-52 cells were cultured in a RPMI medium (Life Technologies, Breda, The Netherlands), supplemented with 10% of fetal calf serum (FCS) and 100 mM glutamine (Life Technologies, Breda, The Netherlands) at 37°C in a humidified atmosphere with 5% CO_2. Cells were washed with saline, trypsinized, washed in RPMI + 10% FCS, and 1×10^7 cells (volume 0.2 mL) were injected subcutaneously (s.c.) into the right flank of 8–10 week-old RNU nude rats (Charles River Laboratories, Wilmington, MA). The biodistribution experiments were initiated 14–20 days after the inoculation of tumor cells (mean tumor weight 0.12 ± 0.04 g). All animal experiments were approved by the Animal Experiments Committee of the University Medical Center at Nijmegen, and were performed in accordance with their guidelines.

Imaging

After an i.v. injection of 4 MBq ^{111}In-DTPA-cG250 (n = 6), rats were anesthetized with a mixture of nitrous oxide/oxygen/isoflurane and placed prone on the parallel-hole, medium-energy collimator of a gamma camera (Orbiter, Siemens Medical Systems, Inc., Hoffman Estates, IL). Images were recorded with a preset count of 300,000 counts at 5 minutes and 24, 48, and 72 hours postinjection (p.i.). The images were digitally stored in a 256×256 matrix.

After an i.v. injection of 20 MBq ^{89}Zr-Df-cG250 (n = 8), rats were anesthetized and placed prone in a PET scanner (ECAT EXACT, Siemens/CTI, Knoxville, TN) (Radical and transaxial resolutions are 5.4 and 6.0 mm, respectively, at full width at half maximum at the center of the field of view). Emission images were recorded at 5 minutes (recording time (r.t.) 8 minutes), and 24 (r.t. 10 minutes), 48 (r.t. 12 minutes), and 72 hours p.i. (r.t. 16 minutes) in 3D mode. Each emission scan was followed by a 5-minute transmission scan with a ^{68}Ge rod-source (2D mode). The cG250 antibody protein dose was always between 50 and 100 μg/rat.

After an i.v. injection with 4 MBq [^{18}F]FDG (n = 7), rats were placed prone in the PET scanner and images were recorded at 1 hour p.i. (total r.t. 20 minutes in 3D mode). From the time of the [^{18}F]FDG injection until the completion of the PET scan, the rats were sedated with the same mixture of nitrous oxide/oxygen/isoflurane. All recorded PET images were iteratively re-

constructed with ECAT software (version 7.2.1, Siemens/CTI, Knoxville, TN), consisting of 2 iterations, with 16 subsets without recon filtering.

Biodistribution Experiments

At the end of each imaging experiment, at 2 hours p.i. of [^{18}F]FDG or 72 hours p.i. of ^{111}In- and ^{89}Zr-labeled cG250, the rats were killed with a lethal dose of sodium pentobarbital. Blood samples, muscle, tumor, lung, spleen, kidney, liver, and small intestine samples were collected. The dissected tissues were weighed and counted in a gamma counter (1480 Wizard 3″, PerkinElmer Life Sciences, Boston, MA). To correct for radioactive decay, injection standards were counted simultaneously. The activity in the samples was expressed as the percentage of injected dose per gram of tissue (%ID/g).

Statistical Analysis

Statistical analysis was performed, using the nonparametric (Kruskal-Wallis) repeated measures one-way analysis of variance (ANOVA). Differences were considered significant when $p < 0.05$, two-sided. If $p < 0.05$, Dunn's multicomparison procedure was performed, selecting only relevant pairs for testing. All values are expressed as the mean ± standard deviation (s.d.).

RESULTS

Conjugation, Radiolabeling, and Quality Control

Approximately one *N*-sucDf moieties or two SCN-Bz-DTPA were conjugated per cG250 IgG molecule. The specific activity of both ^{89}Zr-Df-cG250 and ^{111}In-DTPA-cG250 was 0.4 MBq/μg. At the time of i.v. injection, the radiochemical purity of ^{89}Zr-Df-cG250 and ^{111}In-cG250 was 97.4% and 98.5%, respectively. The immunoreactivity at infinite antigen excess of both preparations exceeded 95%. FPLC analysis of the preparations after incubation in human plasma indicated that both radiolabeled cG250 preparations exhibited high *in vitro* stability: During 4 days of incubation, less than 10% of the ^{89}Zr and ^{111}In radiolabel was released from the moAb.

Imaging

As shown in Figure 1, [^{18}F]FDG did not accumulate in the SK-RC-52 RCC tumors sufficiently to visualize the tumors with [^{18}F]FDG-PET. In contrast, in rats injected with ^{89}Zr-Df-cG250 from 24 hours p.i. onwards, the small tumors were visualized with PET (Fig. 2). Images improved with time, and at 72 hours p.i. all tumors

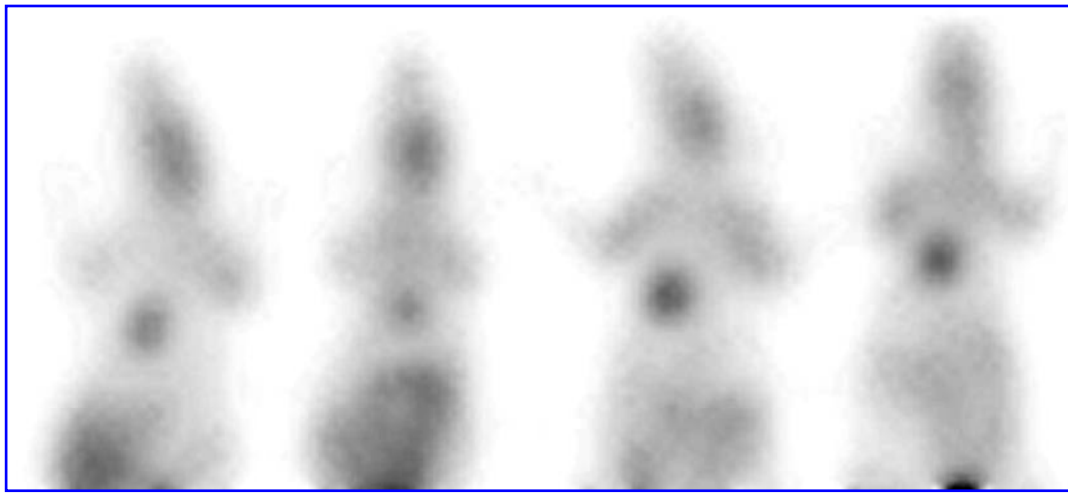

Figure 1. PET anterior projection images of 4 nude rats with SK-RC-52 tumors induced at the right foreleg at 1 hour after an i.v. injection of [^{18}F]FDG. No uptake was observed in the tumors. Note the heart uptake in the rats (arrow). Variable uptake in this organ is also found in humans.

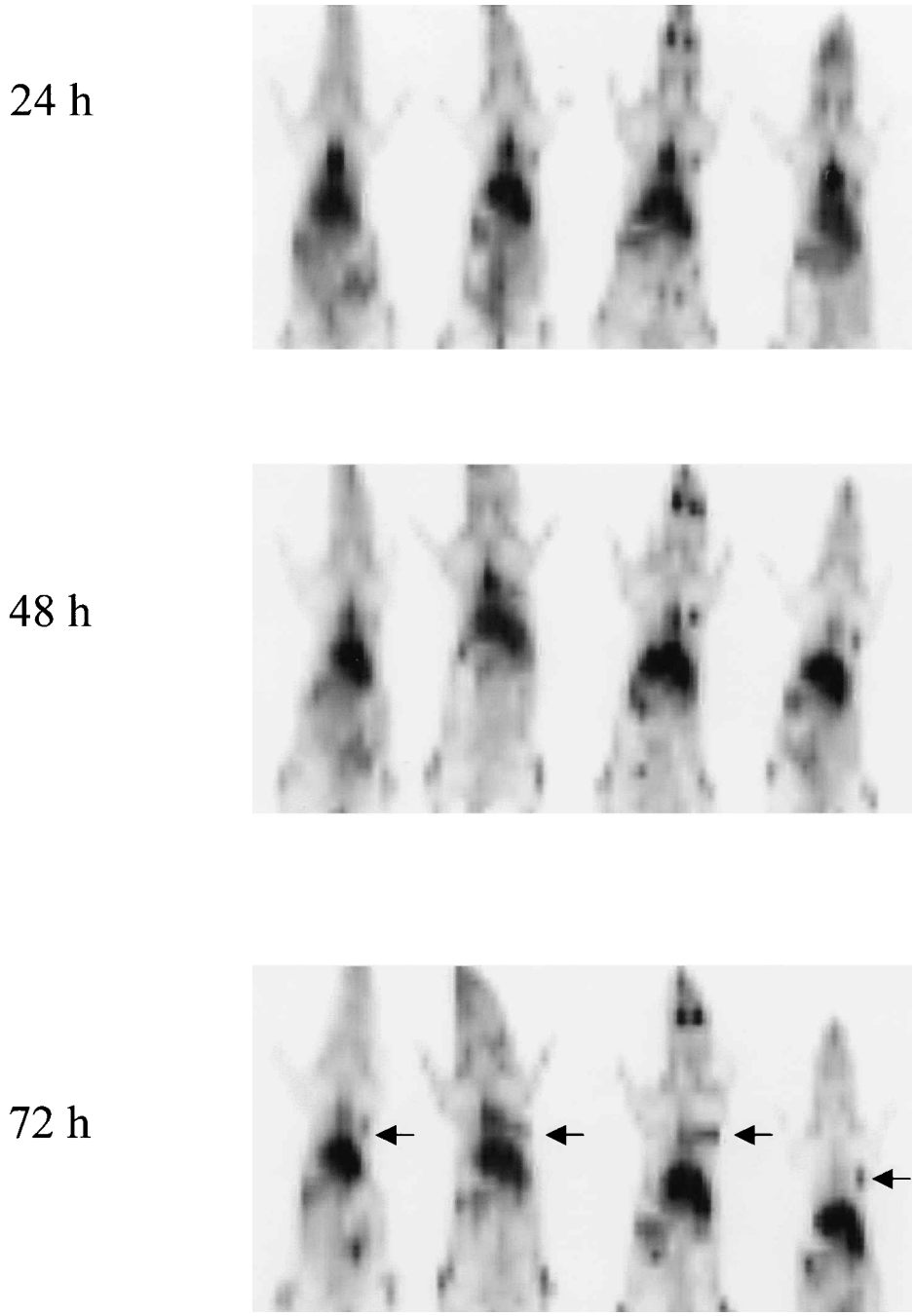

Figure 2. PET anterior projection images of 4 nude rats with SK-RC-52 tumors at the right shoulder at 24, 48, and 72 hours after an i.v. injection of ^{89}Zr-Df-cG250. Five (5) minutes after injection, tumors were not visualized (images not shown). At 24 hours postinjection (p.i.), three RCC tumors were visualized (rat #2–4), whereas, from 48 hours p.i. onwards, tumors were visualized in all rats (arrows). One rat showed a remarkable uptake in the vicinity of the eyes, most likely the result of a local inflammatory response.

were visualized (Fig. 2). The planar images of the rats injected with ^{111}In-DTPA-cG250 are shown in Figure 3. From 24 hours onwards, tumors were clearly visualized, and at later time points, images improved.

Biodistribution Experiments

The biodistribution of [^{18}F]FDG at 2 hours p.i., and of ^{89}Zr-Df-cG250 and ^{111}In-DTPA-cG250 at 3 days p.i. is summarized in Figure 4. In accor-

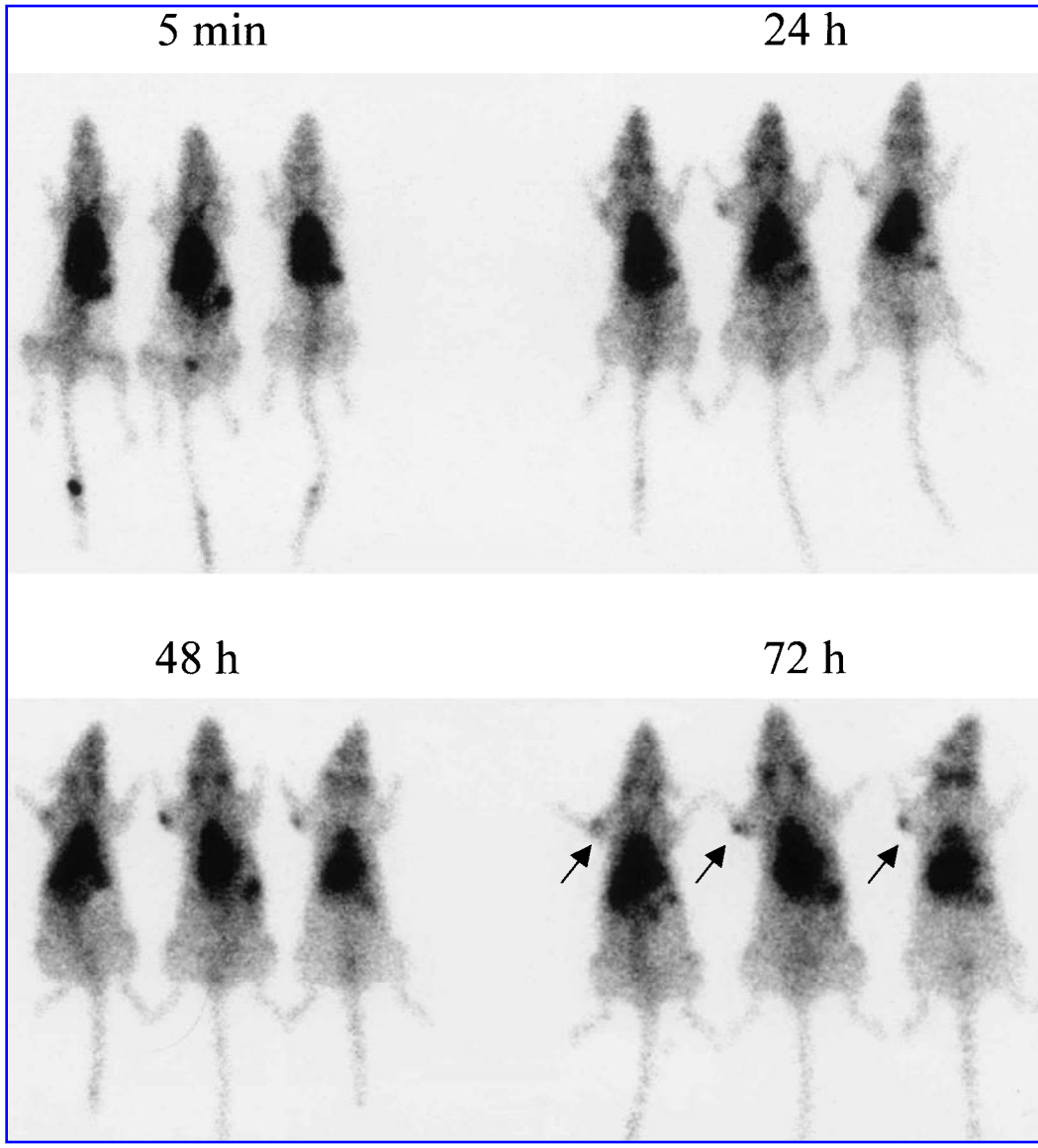

Figure 3. Scintigraphic images of three rats with SK-RC-52 tumors induced at the right shoulder at 5 minutes, and 24, 48, and 72 hours after an i.v. injection of ^{111}In-DTPA-cG250. From 24 hours p.i. onwards, the RCC tumors are visualized (arrow).

dance with the imaging results, no enhanced uptake of [^{18}F]FDG in the SK-RC-52 tumor could be demonstrated, as tumor uptake (0.5 ± 0.1 %ID/g) did not differ significantly from the uptake in the muscle (0.4 ± 0.2 %IDg), or various other organs (Fig. 4).

In contrast, in the rats that received ^{89}Zr- or ^{111}In-labeled cG250, the uptake in the tumor was higher than in any other tissue (5.0 ± 2.4 %ID/g and 4.9 ± 2.9 %ID/g, respectively). Because the activity in the blood was not significantly different in the two groups of rats, tumor-to-blood ratios were similar (3.1 for ^{89}Zr-Df-cG250, and 2.9 for ^{111}In-DTPA-cG250). Also, activity in other normal tissues was not significantly different between the two radiolabeled cG250 groups.

DISCUSSION

This study showed that ^{89}Zr-labeled moAb cG250 can be used for immuno-PET of RCC tumors. Even without the use of a dedicated animal PET camera, relatively small tumors of

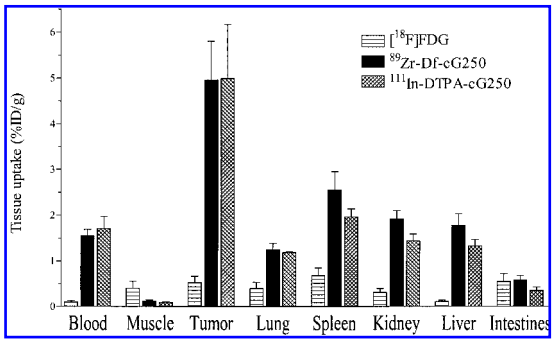

Figure 4. Biodistribution of [^{18}F]FDG (n = 7), ^{89}Zr-Df-cG250 (n = 8), and ^{111}In-DTPA-cG250 (n = 6) in nude rats with subcutaneous (s.c.) SK-RC-52 RCC tumors at 2 hours p.i. ([^{18}F]FDG) or 72 hours p.i. (^{89}Zr- and ^{111}In-labeled cG250).

approximately 100 mg were visualized with ^{89}Zr-Df-cG250 from 24 hours p.i. onward. In general, the maximum accretion of intact radiolabeled moAbs in tumors is reached several days after i.v. injection. In this study, the most optimal images were acquired at 72 hours p.i. of ^{89}Zr-Df-cG250. Furthermore, our data showed that the radioimmunoconjugate was stable in human serum and that the immunoreactivity of radiolabeled moAb cG250 was preserved.

We compared the imaging potential and biodistribution of ^{89}Zr-Df-cG250 immuno-PET with that of ^{111}In-DTPA-cG250 RIS. As with ^{89}Zr-Df-cG250, the s.c. RCC xenografts were well visualized with ^{111}In-DTPA-cG250 from 24 hours p.i. onwards, and the quality of the RCC tumor image improved with time. The uptake of ^{89}Zr-Df-cG250 in the tumor was as high as that of ^{111}In-DTPA-cG250, while the uptake of both radiolabels in normal tissues was similar. Regarding tumor visualization, the PET images of ^{89}Zr-Df-cG250 were at least as informative as the images obtained with ^{111}In-DTPA-cG250. Obviously, the PET images of the rats are suboptimal, because no small animal PET camera with a gantry of a small diameter was available. In both ^{89}Zr-Df-cG250 and ^{111}In-DTPA-cG250 images, a relatively high uptake was seen in the liver, the spleen, and in the heart. In patients, frequent sites of RCC metastases are the lungs (50%–60%) and intraabdominal: the regional lymph nodes and liver (30%–40%), the adrenal gland (20%) and the contralateral kidney (10%).[21] Potentially, small metastases in the upper abdomen can be better detected with 3D PET imaging than with planar whole-body RIS, because with the former technique, specific uptake in RCC lesions may be better delineated from physiological uptake in the surrounding tissues (liver and spleen). Also, potentially immuno-PET can accurately detect small lesions in the lungs, because the resolution of a PET system is higher than the resolution of a gamma camera. The detection rate of pulmonary lesions in RCC patients with ^{131}I-cG250 RIS is disappointingly low.[22]

The uptake of [^{18}F]FDG in the tumor was similar to that in the surrounding tissues and, therefore, the RCC tumors were not visualized with [^{18}F]FDG. In humans, a variable uptake of [^{18}F]FDG in RCC lesions has been reported.[2,22–24] Interestingly, in a direct comparison of RIS with ^{131}I-cG250 and PET imaging with [^{18}F]FDG in patients with metastatic RCC, 70% of the RCC metastases were visualized with [^{18}F]FDG.[22] This relatively low sensitivity of [^{18}F]FDG-PET suggests that at least a part of the RCC lesions has a relatively low [^{18}F]FDG uptake, presumably reflecting a relatively low glucose metabolism. In that study, the sensitivity of ^{131}I-cG250 was even lower (30%). We have recently shown that uptake of cG250 labeled with the residualizing metallic radionuclides (e.g., ^{111}In, $^{88/90}$Y, and ^{177}Lu) in RCC lesions is higher than that of ^{131}I-cG250.[25,26] Therefore, with a residualizing radionuclide, potentially higher radiation doses can be guided to RCC lesions in RIT with moAb cG250.[25,26] The fact that, in this study, the uptake of ^{89}Zr-Df-cG250 in the tumor was identical to that of ^{111}In-DTPA-cG250 confirms that ^{89}Zr should also be classified as a residualizing radionuclide. Thus, the combination of 3D PET imaging and the use of a metallic radionuclide labeled to cG250 (immuno-PET imaging with ^{89}Zr-Df-cG250) could improve the detection rate of metastatic lesions in RCC patients.

In general, with immuno-PET presumably smaller lesions can be visualized, and a more exact localization of the metastases can be given as a result of the improved spatial resolution of PET imaging over single photon imaging with a gamma camera. Moreover, PET images can be quantitatively analyzed more accurately than planar whole-body or single photon emission computed tomography (SPECT) images, allowing for a more accurate estimation of radiation-absorbed doses in RIT treatment planning.[27] As has been demonstrated, ^{89}Zr-Df-cU36 and ^{88}Y-p-SCN-Bz-DOTA-cU36 showed identical pharmacokinetics and uptake in relevant organs, in-

dicating that ^{89}Zr-labeled moAbs can be used to estimate the radiation doses to relevant organs following an injection of ^{90}Y-labeled moAbs in RIT.[28]

CONCLUSIONS

In summary, the cG250 antibody was stably labeled with the positron-emitter ^{89}Zr. The labeling procedure did not affect the immunoreactivity of the antibody. In the nude rat RCC tumor model, the uptake of ^{89}Zr-Df-cG250 in the tumor was identical to that of ^{111}In-DTPA-cG250 and higher than in all normal tissues tested. As a result, the relatively small tumors were visualized with both ^{111}In-DTPA-cG250 RIS and ^{89}Zr-Df-cG250 immuno-PET, even without the use of a dedicated animal PET camera. Regarding the delineation of uptake in surrounding tissues next to the uptake in normal organs, such as the liver and spleen, the ^{89}Zr-Df-cG250 images were superior to the ^{111}In-DTPA-cG250 images. ^{89}Zr-Df-cG250 PET imaging could improve the detection of metastatic lesions in RCC patients. It can be anticipated that, with immuno-PET, smaller lesions can be visualized and a more exact localization of the metastases can be given as a result of the improved spatial resolution of PET imaging, as compared to single photon imaging. Finally, the more accurate estimates of radiation-absorbed doses that can be obtained with immuno-PET, as compared to RIS with a gamma camera, might be of value in the planning and monitoring of RIT.

ACKNOWLEDGMENTS

This study was supported by the Dutch Cancer Society (KWF), grant number: KUN99-1973. E. Oosterwijk was supported by the Ludwig Institute for Cancer Research, New York, NY. The authors wish to thank P. Kok; Department of Nuclear Medicine, UMC Nijmegen; Nijmegen, The Netherlands, for PET imaging of the rats.

REFERENCES

1. Gambhir SS, Czernin J, Schwimmer J, et al. A tabulated summary of the FDG PET literature. *J Nucl Med* 2001;42:15.
2. Ramdave S, Thomas GW, Berlangieri SU, et al. Clinical role of F-18 fluorodeoxyglucose positron emission tomography for detection and management of renal cell carcinoma. *J Urol* 2001;166:825.
3. Goldberg MA, Mayo Smith WW, Papanicolaou N, et al. FDG-PET characterization of renal masses: Preliminary experience. *Clin Radiol* 1997;52:510.
4. Safaei A, Figlin R, Hoh CK, et al. The usefulness of F-18 deoxyglucose whole-body positron emission tomography (PET) for restaging of renal cell cancer. *Clin Nephrol* 2002;57:56.
5. Verel I, Visser GWM, Boerman OC, et al. Long-lived positron emitters zirconium-89 and iodine-124 for scouting of therapeutic radioimmunoconjugates with PET. *Cancer Biother Radiopharm* 2003;18:655.
6. Meijs WE, Herscheid JD, Haisma HJ, et al. Evaluation of desferal as a bifunctional chelating agent for labeling antibodies with Zr-89. [abstr.] *Int J Rad Appl Instrum* 1992;43:1443.
7. Verel I, Visser GW, Boellaard R, et al. ^{89}Zr immuno-PET: Comprehensive procedures for the production of (89)Zr-labeled monoclonal antibodies. *J Nucl Med* 2003;44:1271.
8. Mealey J. Turnover of carrier-free zirconium-89 in man. *Nature* 1957;179:674.
9. Roselli M, Schlom J, Gansow OA, et al. Comparative biodistributions of yttrium- and indium-labeled monoclonal antibody B72.3 in athymic mice bearing human colon carcinoma xenografts. *J Nucl Med* 1989;30:672.
10. Muller WA, Schaffer EH, Linzner U. Studies on incorporated short-lived beta-emitters with regard to the induction of late effects. *Radiat Environ Biophys* 1980;18:1.
11. Oosterwijk E, Ruiter DJ, Hoedemaeker PJ, et al. Monoclonal antibody G250 recognizes a determinant present in renal-cell carcinoma and absent from normal kidney. *Int J Cancer* 1986;38:489.
12. Steffens MG, Boerman OC, Oosterwijk-Wakka JC, et al. Targeting of renal cell carcinoma with iodine-131-labeled chimeric monoclonal antibody G250. *J Clin Oncol* 1997;15:1529.
13. Grabmaier K, Vissers JL, De Weijert MC, et al. Molecular cloning and immunogenicity of renal cell carcinoma-associated antigen G250. *Int J Cancer* 2000; 85:865.
14. Uemura H, Nakagawa Y, Yoshida K, et al. MN/CA IX/G250 as a potential target for immunotherapy of renal cell carcinomas. *Br J Cancer* 1999;81:741.
15. Pastorekova S, Parkkila S, Parkkila AK, et al. Carbonic anhydrase IX, MN/CA IX: Analysis of stomach complementary DNA sequence and expression in human and rat alimentary tracts. *Gastroenterology* 1997;112:398.
16. Meijs WE, Herscheid JD, Haisma HJ. Production of highly pure no-carrier added ^{89}Zr for the labeling of antibodies with a positron emitter. *Appl Radiat Isot* 1994;45:1143.
17. Ruegg CL, Anderson-Berg WT, Brechbiel MW, et al. Improved *in vivo* stability and tumor targeting of bismuth-labeled antibody. *Cancer Res* 1990;50:4221.
18. Hnatowich DJ, Childs RL, Lanteigne D, et al. The preparation of DTPA-coupled antibodies radiolabeled

with metallic radionuclides: An improved method. *J Immunol Methods* 1983;65:147.
19. Lindmo T, Boven E, Cuttitta F, et al. Determination of the immunoreactive fraction of radiolabeled monoclonal antibodies by linear extrapolation to binding at infinite antigen excess. *J Immunol Methods* 1984;72:77.
20. Ebert T, Bander NH, Finstad CL, et al. Establishment and characterization of human renal cancer and normal kidney cell lines. *Cancer Res* 1990;50:5531.
21. McDougal WS, Garnick MB. Comprehensive textbook of genitourinary oncology. In Vogelzang NJ, Scardino PT, Shipley WU, Coffey DS (Eds.). Lippincott, Williams, and Wilkins, Baltimore, 2000, p. 155.
22. Brouwers AH, Dorr U, Lang O, et al. ^{131}I-cG250 monoclonal antibody immunoscintigraphy versus [^{18}F]FDG-PET imaging in patients with metastatic renal cell carcinoma: A comparative study. *Nucl Med Commun* 2002;23:229.
23. Miyakita H, Tokunaga M, Onda H, et al. Significance of ^{18}F-fluorodeoxyglucose positron emission tomography (FDG-PET) for detection of renal cell carcinoma and immunohistochemical glucose transporter 1 (GLUT-1) expression in the cancer. *Int J Urol* 2002;9:15.
24. Lang O, Brouwers AH, Mergenthaler HG, et al. Value of whole-body ^{18}F-FDG-PET in metastatic renal cell carcinoma—correlation with tumor aggressiveness? *J Nucl Med* 2000;41:117P.
25. Brouwers AH, Buijs WCAM, Oosterwijk E, et al. Targeting of metastatic renal cell carcinoma with the chimeric monoclonal antibody G250 labeled with ^{131}I or ^{111}In: An intrapatient comparison. *Clin Cancer Res* 2003;9(suppl.):3953S.
26. Brouwers AH, van Eerd JEM, Frielink C, et al. Optimization of radioimmunotherapy of renal cell carcinoma: Labeling of monoclonal antibody cG250 with ^{131}I, ^{90}Y, ^{177}Lu, or ^{186}Re. *J Nucl Med* 2004;45:327.
27. Lee FT, Scott AM. Immuno-PET for tumor targeting. *J Nucl Med* 2003;44:1282.
28. Verel I, Visser GW, Boellaard R, et al. Quantitative (89)Zr immuno-PET for *in vivo* scouting of (90)Y-labeled monoclonal antibodies in xenograft-bearing nude mice. *J Nucl Med* 2003;44:1663.

This article has been cited by:

1. Melissa A. Deri, Brian M. Zeglis, Lynn C. Francesconi, Jason S. Lewis. 2012. PET imaging with 89Zr: From radiochemistry to the clinic. *Nuclear Medicine and Biology* . [CrossRef]
2. Arutselvan Natarajan, Frezghi Habte, Sanjiv S. Gambhir. 2012. Development of a Novel Long-Lived ImmunoPET Tracer for Monitoring Lymphoma Therapy in a Humanized Transgenic Mouse Model. *Bioconjugate Chemistry* 120611160123008. [CrossRef]
3. Guus A. M. S. Dongen, Alex J. Poot, Danielle J. Vugts. 2012. PET imaging with radiolabeled antibodies and tyrosine kinase inhibitors: immuno-PET and TKI-PET. *Tumor Biology* . [CrossRef]
4. Danielle J. Vugts, Guus A.M.S. van Dongen. 2012. 89Zr-labeled compounds for PET imaging guided personalized therapy. *Drug Discovery Today: Technologies* . [CrossRef]
5. Sukhwinder Kaur, Ganesh Venktaraman, Maneesh Jain, Shantibhusan Senapati, Pradeep K. Garg, Surinder K. Batra. 2011. Recent trends in antibody-based oncologic imaging. *Cancer Letters* . [CrossRef]
6. Brian M Zeglis, Priya Mohindra, Gabriel I Weissmann, Vadim Divilov, Scott Alan Hilderbrand, Ralph Weissleder, Jason S. Lewis. 2011. A Modular Strategy for the Construction of Radiometallated Antibodies for Positron Emission Tomography Based on Inverse Electron Demand Diels-Alder Click Chemistry. *Bioconjugate Chemistry* 110831040206032. [CrossRef]
7. Jun Toyohara, Kiichi Ishiwata. 2011. Animal tumor models for PET in drug development. *Annals of Nuclear Medicine* . [CrossRef]
8. Rozemarie Gilles, Lioe-Fee Geus-Oei, Peter F. A. Mulders, Wim J. G. Oyen. 2011. Immunotherapy response evaluation with 18F-FDG-PET in patients with advanced stage renal cell carcinoma. *World Journal of Urology* . [CrossRef]
9. Derrek A. Heuveling, Remco de Bree, Guus A.M.S. van Dongen. 2011. The potential role of non-FDG-PET in the management of head and neck cancer. *Oral Oncology* **47**:1, 2-7. [CrossRef]
10. Brian M. Zeglis, Jason S. Lewis. 2011. A practical guide to the construction of radiometallated bioconjugates for positron emission tomography. *Dalton Transactions* **40**:23, 6168. [CrossRef]
11. Guus A.M.S. van Dongen , Maria J.W.D. Vosjan . 2010. Immuno-Positron Emission Tomography: Shedding Light on Clinical Antibody Therapy. *Cancer Biotherapy & Radiopharmaceuticals* **25**:4, 375-385. [Abstract] [Full Text HTML] [Full Text PDF] [Full Text PDF with Links]
12. Nathan Lawrentschuk, Ian D. Davis, Damien M. Bolton, Andrew M. Scott. 2010. Functional imaging of renal cell carcinoma. *Nature Reviews Urology* **7**:5, 258-266. [CrossRef]
13. Maria J W D Vosjan, Lars R Perk, Gerard W M Visser, Marianne Budde, Paul Jurek, Garry E Kiefer, Guus A M S van Dongen. 2010. Conjugation and radiolabeling of monoclonal antibodies with zirconium-89 for PET imaging using the bifunctional chelate p-isothiocyanatobenzyl-desferrioxamine. *Nature Protocols* **5**:4, 739-743. [CrossRef]
14. Andreas Helisch, Oliver Thews, Hans-Georg Buchholz, Julia Tillmanns, Andrea Kronfeld, Laura M. Schreiber, Mathias Schreckenberger, Peter Bartenstein. 2010. Small animal tumour imaging with MRI and the ECAT EXACT scanner: application of partial volume correction and comparison with microPET data. *Nuclear Medicine Communications* **31**:4, 294-300. [CrossRef]
15. Lars R. Perk, Maria J. W. D. Vosjan, Gerard W. M. Visser, Marianne Budde, Paul Jurek, Garry E. Kiefer, Guus A. M. S. Dongen. 2010. p-Isothiocyanatobenzyl-desferrioxamine: a new bifunctional chelate for facile radiolabeling of monoclonal antibodies with zirconium-89 for immuno-PET imaging. *European Journal of Nuclear Medicine and Molecular Imaging* **37**:2, 250-259. [CrossRef]
16. Jason P. Holland, Yiauchung Sheh, Jason S. Lewis. 2009. Standardized methods for the production of high specific-activity zirconium-89. *Nuclear Medicine and Biology* **36**:7, 729-739. [CrossRef]

17. Ludwig Dubois, Natasja G. Lieuwes, Alfonso Maresca, Anne Thiry, Claudiu T. Supuran, Andrea Scozzafava, Bradly G. Wouters, Philippe Lambin. 2009. Imaging of CA IX with fluorescent labelled sulfonamides distinguishes hypoxic and (re)-oxygenated cells in a xenograft tumour model. *Radiotherapy and Oncology* **92**:3, 423-428. [CrossRef]
18. R MEIER, M PIERT, G PIONTEK, M RUDELIUS, R OOSTENDORP, R SENEKOWITSCHSCHMIDTKE, T HENNING, W WELS, C UHEREK, E RUMMENY. 2008. Tracking of [18F]FDG-labeled natural killer cells to HER2/neu-positive tumors. *Nuclear Medicine and Biology* **35**:5, 579-588. [CrossRef]
19. S PERMPONGKOSOL, M NIELSEN, S SOLOMON. 2006. Percutaneous renal cryoablation. *Urology* **68**:1, 19-25. [CrossRef]
20. NATHAN LAWRENTSCHUK, IAN D. DAVIS, DAMIEN M. BOLTON, ANDREW M. SCOTT. 2006. Positron emission tomography (PET), immuno-PET and radioimmunotherapy in renal cell carcinoma: a developing diagnostic and therapeutic relationship. *BJU International* **97**:5, 916-922. [CrossRef]
21. W Kimryn Rathmell, Tricia M Wright, Brian I Rini. 2005. Molecularly targeted therapy in renal cell carcinoma. *Expert Review of Anticancer Therapy* **5**:6, 1031-1040. [CrossRef]